RSC Advances

PAPER

View Article Online
View Journal | View Issue

Cite this: *RSC Adv.*, 2018, **8**, 22635

Extracellular polymeric substances (EPS) secreted by *Purpureocillium lilacinum* strain Y3 promote biosynthesis of jarosite

Peng Bao,[a] Mingchen Xia,[a] Ajuan Liu,[a] Mingwei Wang,[a] Li Shen,[ab] Runlan Yu,[ab] Yuandong Liu,[ab] Jiaokun Li,[ab] Xueling Wu,[ab] Caoming Fang,[c] Miao Chen,[de] Guanzhou Qiu[ab] and Weimin Zeng*[abc]

In this study, the biosynthesis of jarosite by *Purpureocillium lilacinum* was investigated. Firstly, we found when the pH value was lower than 2.50 at 30 °C, the concentration of Fe^{3+} in the solution significantly dropped about 72% after inoculation and a yellow-ocher precipitate was observed on the mycelium surface. X-ray diffraction analysis revealed the precipitate was jarosite. Thereafter, the characterization of the biomineralization process by scanning electron microscopy showed that mineral precipitates started on the cell surface, and then thoroughly covered it. Furthermore the effect of extracellular polymeric substances (EPS) on the biosynthesis of jarosite was investigated. The results suggested Fe^{3+} only dropped 5.2% in 2 days when EPS were stripped. Finally, through monitoring the changes of mycelium surface groups by Fourier transform infrared spectroscopy, we found the biomineralization process originated from the existence of free P=O groups in EPS which acted as crystallization nuclei to promote $Fe(OH)_3$ transformation into jarosite by the formation of P–O–Fe bonds.

Received 10th April 2018
Accepted 6th June 2018

DOI: 10.1039/c8ra03060j

rsc.li/rsc-advances

1 Introduction

Biomineralization is the process in which inorganic elements selectively deposit on the surface of special organic matters from the environment with the participation of organisms. The compositions of biominerals are varied and calcium-containing minerals are among the most common forms, making up almost half the total biominerals. Besides, silicon and iron oxide also take a great percentage.[1,2] Among them, the naturally occurring jarosite is usually connected with microbial action. The general formula of jarosite is $KFe_3(SO_4)_2(OH)_6$, which is a hydrated iron-potassium sulfate and is stabilized at low pH value.[3,4] Only at a pH value lower than 4 can jarosite be formed.[5] The typical method of jarosite generation is the reaction of Fe-rich rocks with acid oxidized fluids or the oxidation of pyrite-rich rocks.[6] Besides, jarosite has been found on sediments at Mawrth Vallis and Meriadiani Planum on the surface of Mars.[7,8]

Acid mine drainages (AMD) with high concentration of ferric ions and sulfates is one of the most typical pollutants in the mine environment. The process of biosynthesis of jarosite can contribute to shape and control the geochemical properties of this environment by removing ferric ions more efficiently.[9] Furthermore, biological nanoparticles of jarosite possess the advantage of milder process condition and absence of toxic chemicals, and showed the good performance for pigment in the painting and adsorbing material in the treatment of waste water.[10,11]

Biomineralization can be classified to biologically induced mineralization (BIM) and biologically controlled mineralization (BCM).[12] In BIM process, mineralization happens when the organism modifies its local microenvironments by cellular components just like EPS, cytoderm and some spores, which possess charged surface, which can serve as adsorption sites to interact with metal ions bringing about growth and nucleation of minerals. In this case, the organism does not exert any control over the mineralization process. In BCM process, the mineralization is not influenced by various environmental factors, and the deposition process of mineral is tightly regulated by organism. The mineral formed by this method contains a large number organic matter, and the shape of mineral is homogeneous. But in BCM process the biomass inflicts a high level of control over the nucleation and growth of minerals, and this process usually takes place inside the cell.[13] Besides, the ratio of Fe^{2+}/Fe^{3+}, the concentration of Fe^{3+} and the pH value are essential elements of the biomineralization of jarosite despite the nucleation sites by themselves are enough to facilitate jarosite formation.[14]

[a]*School of Minerals Processing and Bioengineering, Central South University, Changsha 410083, China. E-mail: zengweimin1024@126.com; Tel: +86-13787288594*
[b]*Key Laboratory of Biometallurgy, Ministry of Education, Changsha 410083, China*
[c]*China Nonferrous Metal Mining (Group) Co., Ltd, Beijing, China*
[d]*CSIRO Process Science and Engineering, Clayton, Victoria 3168, Australia*
[e]*Centre for Advanced Materials and Industrial Chemistry, RMIT University, Melbourne 3000, Australia*

Biomineralization in artificial and natural environments by prokaryotic microorganism has been widely investigated.[15,16] For example, Bontognali *et al.* reported that bacteria *D. brasiliensis* can intervene in chaotic Ca-dolomite and Mg-calcite mineralization through metabolic activity mediating this process in artificial environment, and the mechanism is independent and induces supersaturation and the following mineralization of carbonate.[17] As the study of the environment of acid mine drainages (AMD) progressed, we find out that the eukaryotes also play an important role to keep the stability of the ecosystem.[18] Oggerin *et al.* reported that an acidic fungus *Purpureocillium lilacinum* was separated from the banks of the Río Tinto basin, which may play a significant role in specifically precipitating jarosite in natural extreme acidic ecosystems, the ability is limited to specific species and not universal to all fungi isolated from this acidic surroundings.[19]

Extracellular polymeric substances (EPS) of microorganism play an important influence on biofilm formation, bacteria transport and adhesion, heavy metal ions accumulation and biomineralization.[20–22] The role of EPS on biomineralization usually be classified to electrostatic interaction and charge accumulation, geometric matching of crystal, and complementary structure in space.[23–25] For example, the sulphate-reducing bacteria (SRB) may induce mineral precipitation by mediating the pH value or affect the composition of mineral by generating a fundamental organic matrix. The existence of EPS generated by specific microorganisms is obviously of crucial significance for incorporating Mg^{2+} into the mineral lattice.[17] Besides, it is reported that the EPS constituting the microbial mats developed along the coastal sabkhas of Abu Dhabi are indispensable components for the formation of dolomite.[26] Moreover, the formation of Fe–O–P bonds between goethite surface and phosphoryl groups is the way of EPS-goethite specific interaction, which offers a forceful bonding method and contributes to microorganisms conglutination leading to biofilm formation and cell immobilization in the near-surface ecosystem.[27] Even though the significance of microorganisms for mineralization is generally admitted, the exact mechanism in the formation process remains unclear.

In the present study, the eukaryotes *P. lilacinum* strain Y3 was used to investigate the biosynthesis ability of jarosite. Then the EPS of microorganism was stripped by several methods to analyze the effect of EPS deficiency on biomineralization. Finally, Fourier transform infrared spectroscopy (FTIR) analysis during biomineralization process was conducted to reveal the mechanism of biosynthesis of jarosite by *P. lilacinum* strain Y3.

2 Materials and methods

2.1 Fungal strain and growth conditions

P. lilacinum strain Y3, an acidic fungus, was obtained from Key Laboratory of Biometallurgy of Ministry of Education (Central South University, China). The fungus was cultured on potato dextrose agar (PDA, 3.9% (w/v)) slant and incubated for 7 days at 30 °C. Then sterilized water was used to wash the mature conidia from the surface of PDA slant. The number of spores was counted using a Neubauer counting chamber under an optical microscope and the spore suspension was adjusted to a final concentration of 10^7 spores per mL.

To culture in liquid medium, 1 mL of spore suspension was inoculated into 250 mL Erlenmeyer flasks containing 100 mL medium comprised of 5 g L^{-1} sucrose, 5 g L^{-1} yeast extract and 5 g L^{-1} malt extract. The flasks were incubated in a rotary shaker at 30 °C and 120 rpm.

2.2 Biomineralization experiments

The fungus was cultured in Erlenmeyer flasks at 30 °C for 2 days and enough mycelium pellets formed. The biomass was collected by centrifugation at 3000 rpm for 10 min. Then 10 g of wet fungal biomass was added to 100 mL of metal-containing solution (0.5 M L^{-1} ferric sulfate stock solution and 1 M L^{-1} potassium sulfate stock solution were added until the initial concentrations of Fe^{3+} and K^+ were adjusted to 0.02 and 0.1 M L^{-1}, respectively). Control experiments were conducted without fungal biomass. Incubation was continued for 11 days at 30 °C and 120 rpm in the rotary shaker, until the concentration of metal ions in solution remained stable. The 5 M L^{-1} potassium hydroxide solution was used to adjust the pH value of the solutions. Experiments were carried out in triplicate.

2.3 EPS extraction with different methods

At present, few studies concerning with extraction methods of fungal EPS have been reported, so different methods of extracting EPS from *P. lilacinum* were carried out to investigate the importance of fungal EPS in biomineralization process. The detail experimental procedures are illustrated in Fig. 1. The results indicated that a comprehensive method of vibration combining with formaldehyde and NaOH could achieve the highest EPS yield, followed by ultrasonic method, and autoclaved method was the worst (data not shown). Then 10 g of wet fungal biomass, which the EPS have been stripped, was added to 100 mL of metal-containing (0.02 M L^{-1} Fe^{3+} and 0.1 M L^{-1} K^+) solution (pH 2.5). Then the solution was cultured for 11 days at 30 °C and 120 rpm, in the rotary shaker.

2.4 Analysis methods

Ferric iron concentration in solution was assayed by 1,10-phenanthroline spectrophotometry.[28] Polysaccharide content in EPS was measured by the phenol-sulfuric acid method with glucose as the standard.[29] The amount of proteins was determined by the BCA Protein Assay Kit using bovine serum albumin as the standard.[30] The pH value was determined by pH S-3C acid meter after calibrating with standard buffer solution. The micromorphology of fungal mycelium pellets during biomineralization process was observed by scanning electron microscope (SEM) (Tescan Vega3) and the composition of elements was characterized by Energy Dispersive X-ray Detector (EDX). The crystal phases of biomineral were assayed by X-ray diffraction (XRD) (Leco CS744). The functional groups of *P. lilacinum* before and after biomineralization were examined by Fourier transform infrared spectroscopy (FTIR) (NEXUS 670), the spectra range were 4000–400 cm^{-1} and the samples were prepared as KBr discs.

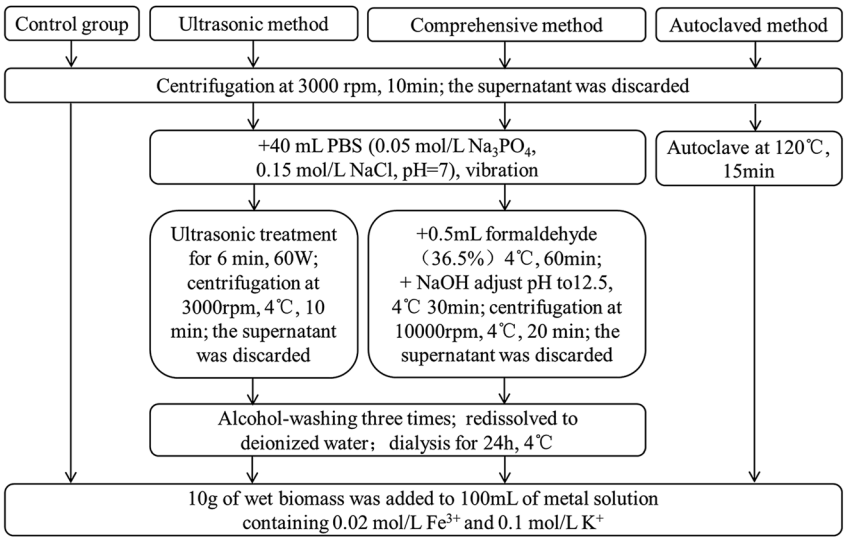

Fig. 1 Flow chart of EPS extraction with different methods.

3 Results and discussion

3.1 Effect of *P. lilacinum* on biomineralization

3.1.1 Inoculating with *P. lilacinum* increased de-ironing efficiency. The effect of pH on the de-ironing efficiency with and without *P. lilacinum* was shown in Fig. 2, and it could be seen that the efficiency obviously increased when inoculating with *P. lilacinum*. When the pH value was 2.10 and 2.30 (Fig. 2A and B), the color of mycelium pellet turned to yellow-ocher and the concentration of Fe^{3+} in the medium dropped about 71.1% and 72.3% respectively in 11 days. But in the control experiments without cells, the concentration of Fe^{3+} nearly did not change, despite the same initial content of Fe^{3+} and pH value of the medium. When the pH value was 2.50 with the inoculation

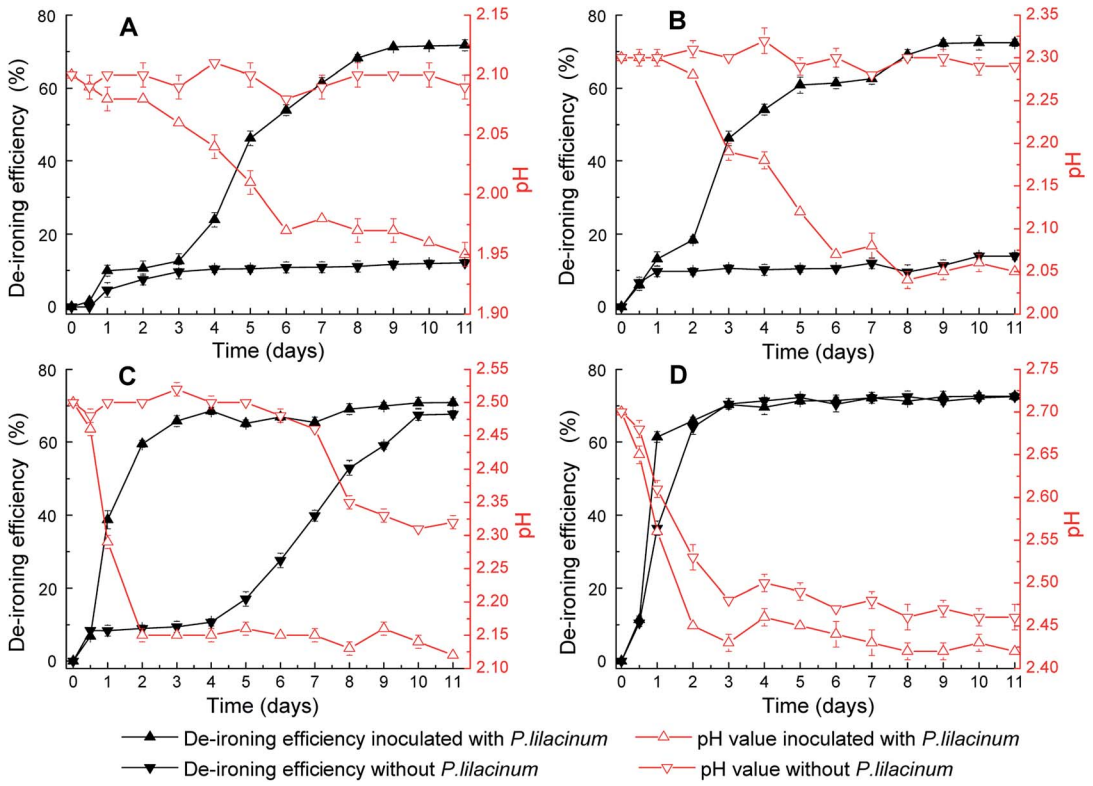

Fig. 2 The variation of setting efficiency of Fe^{3+} and pH value over time during biomineralization process induced *P. lilacinum* at different initial pH: (A) pH 2.1; (B) pH 2.3; (C) pH 2.5; (D) pH 2.7.

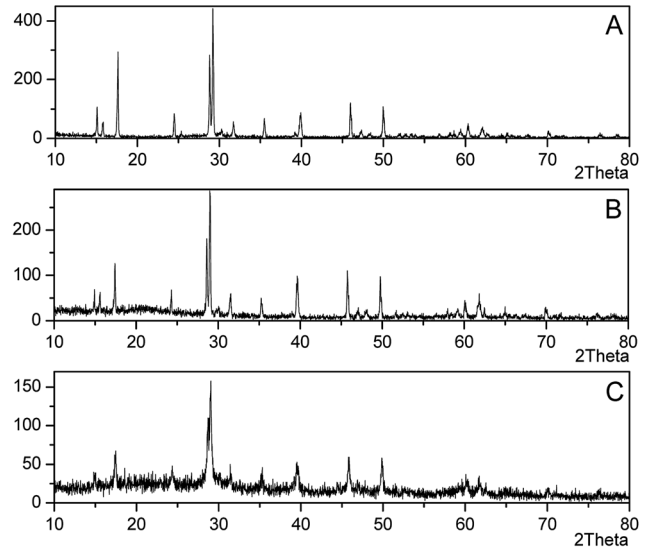

Fig. 3 XRD patterns of jarosite and fungal induced mineral (pH 2.5, 11th day): (A) Jarosite XRD standard pattern (PDF#22–0827); (B) XRD pattern of mineral formed in control experiments without cells; (C) XRD pattern of mineral induced by *P. lilacinum* Y3.

of *P. lilacinum* (Fig. 2C), only in 3 days, the mycelium surface obviously turned to yellow-ocher and the concentration of Fe^{3+} dropped about 71.5%, and no precipitation was observed on the bottom of flasks. In the control experiment, the setting process of Fe^{3+} was very slow, and it increased after the 3rd day. However, when the pH value was 2.70 (Fig. 2D), only in 1 day, the precipitation was clearly observed on the bottom of flasks with or without inoculation and the concentration of Fe^{3+} dropped about 73.2% and 72.5% respectively. These results indicated that improving pH value would obviously increase the hydrolysis tendency of Fe^{3+}.

The yellow-ocher colored precipitate in mycelium surface was analyzed by XRD as jarosite (Fig. 2A–C), and the precipitate on the bottom of flasks was analyzed as $Fe(OH)_3$ (Fig. 2D). Fig. 3 showed the XRD patterns of jarosite induced by *P. lilacinum*. The XRD analysis undisputedly verified that the yellow-ocher coloured precipitate on the mycelium surface belonged to jarosite. But the crystallinity of the precipitates which obtained by different methods differed on the basis of diffraction peaks of the crystal plane.[31] The well-recognized and forceful peaks of the precipitate got by control experiments (without cells) indicated that they accord with well-crystallized phases (Fig. 3B). But the precipitate got by biomineralization process showed an obvious amorphous noise in the background (Fig. 3C). What is more, the decrease of pH occurred in experiments with or without inoculation, the variation tendency was exactly consistent to the variation of the concentration of Fe^{3+}. The decrease of pH could be due to H^+ was generated in the hydrolysis and mineralization step.[32]

The mineralization process was obviously restrained by acidity. It was clearly observed from Fig. 2 that pH value in the solution played a crucial part in the balance of mineral precipitate and dissolution, and high energy was necessary for activating the new phase.[33] As could be seen in the Fig. 2A, the de-ironing efficiency without *P. lilacinum* was significantly restrained at lower pH value. This change rule was alike to the patterns in Fig. 2B and C. Furthermore, setting efficiency of Fe^{3+} significantly increased when inoculated with *P. lilacinum* in all four experimental groups. These results proved that inoculating with *P. lilacinum* could reduce the dependence of mineralization process upon pH value and could facilitate mineral growth. What's more, as Fig. 2D showed higher setting efficiency of Fe^{3+} was got with improving pH value. While at higher initial pH values, the change of concentration of Fe^{3+} due to biomineralization cannot be distinguished from hydrolysis because the Fe^{3+} hydrolyzes more rapidly.[34] Besides, Fig. 2C showed no obvious change in eventual efficiency at the same equilibrated pH value. So, the discrepancy of iron-removal efficiency in Fig. 2 was attributed to the different synthetic rate of mineral. But, when the initial pH value was adjusted to 2.50, the effect of *P. lilacinum* in setting efficiency of Fe^{3+} was most obvious.

3.1.2 SEM-EDX analysis during biosynthesis of jarosite by *P. lilacinum*. The scanning electron microscopy (SEM) images of the mycelium surface were shown in Fig. 4A–D. Along with time, the biomineralization process obviously started on the fungal cell surfaces with the growth of loose cauliflower-like particle, until cell wall was thoroughly covered with mineral precipitate (Fig. 4D). We observed that platelike crystals grew within the mycelium surface and comprised well-developed crystal faces that could be observed (Fig. 4B and C). The energy-dispersive X-ray spectroscopy (EDX) was employed to get information about the elements constitution of the aggregates and coating mineral.[35] The results of EDX spectra showed that the essential elements were C and O (Spectrum 1), which indicated almost no mineral formed in mycelium surface after 12 hours. Over time, in the fungal cell surfaces we could find other elements such as C, O, S, K and Fe (Spectrum 2 and 3). The existence of C indicated that the cells join in the formation of mineral aggregates. The small amount of crystals that formed together with cell surfaces would induce the generation of more mineral precipitate[19]

3.2 The effect of EPS from *P. lilacinum* on the biomineralization

Fig. 5 shows the efficiency of jarosite formation on fungal hyphae surface at pH 2.5 with original and stripped EPS. In the control experiments, the mycelium pellets without treated and the mineral precipitate formed apparently on the surface of mycelium pellets. The concentration of Fe^{3+} dropped about 71.7% after 2 days and the decrease tendency is exponential. While no visible precipitate was observed in the experimental groups with stripped EPS after 2 days. By comprehensive method, the EPS removed most thoroughly and the concentration of Fe^{3+} nearly did not change after 2 days. The subdued variation in slopes of the curves demonstrated that the inductive phase of jarosite formation without EPS was lengthened. These results confirmed that the more complete EPS separation, the lower biomineralization efficiency. What is more, the variation tendency of pH was also consistent to the variation of Fe^{3+}.

In the above discussion, we has known that the efficiency holds steady when the equilibrated pH value and original Fe^{3+}

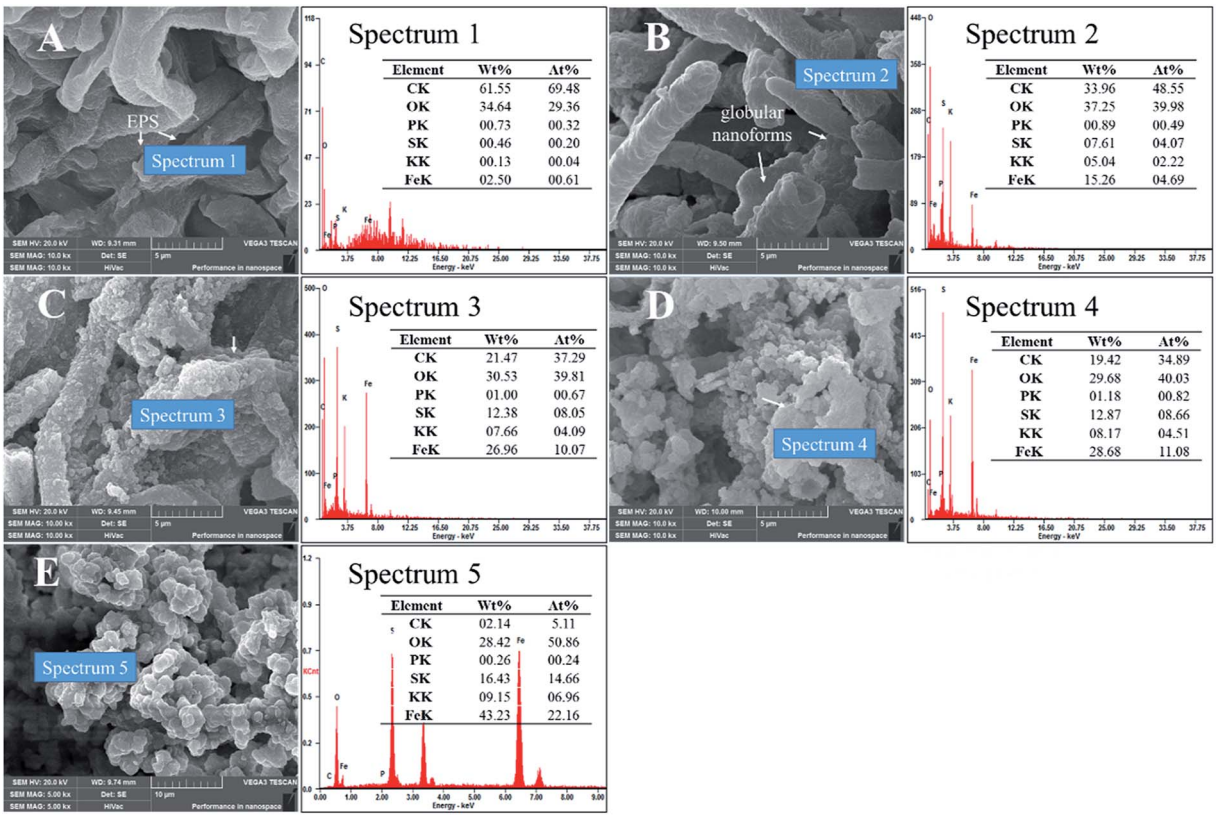

Fig. 4 SEM micrographs analysis showing the biomineralization process in different time (pH 2.5): (A) 12th hour; (B) 1st day; (C) 2nd day; (D) 11th day. And the precipitation of control experiments without cells: (E) 11th day.

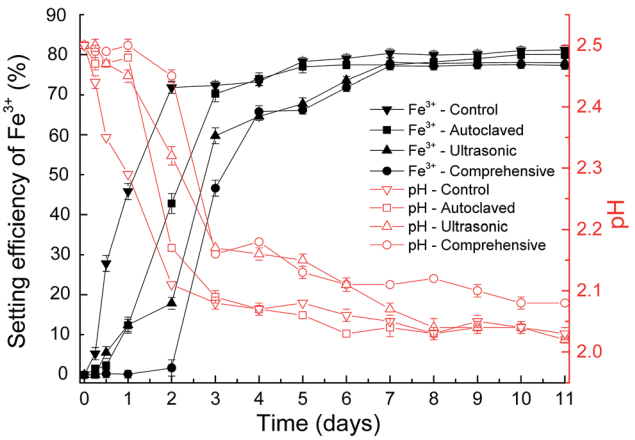

Fig. 5 The variation of pH value and biomineralization efficiency during biosynthesis of jarosite by *P. lilacinum* with and without EPS at pH 2.5.

concentration are same, nucleation sites decide the balanced reflection time. As the curves of time and setting efficiency of Fe^{3+} showed, the existence of EPS could shorten induction period and bring the reaction to equilibrium more rapidly. It is apparent that the EPS is significantly important for jarosite formation.

After standing for 2 days, the mineralized mycelium pellets were obtained after filtering of the solutions and identified by SEM. Fig. 6A–C showed the SEM images of biomineralization by different methods to strip EPS. Stripping EPS by autoclaved method was shown in Fig. 6A, the precipitate of jarosite covered all the biomass. The stoichiometric proportion of the mineral globular aggregates matched those of jarosite (Spectrum 1). But the trace of EPS was not prominent, and no platelike crystals grew. Stripping EPS by ultrasonic method was shown in Fig. 6B. Unformed pellets with uneven size and some emplastic substances were observed on the surface of mycelium. The EDX analysis result showed that the atom ratio of S to Fe was about 1 : 1, indicating that only a part of $Fe(OH)_3$ transformed into mineral precipitate (Spectrum 2).[33] Stripping EPS by comprehensive method was shown in Fig. 6C. The EPS removed most thoroughly in this method and the mycelium surface was smooth, no viscous substance and amorphous grains could be detected in this condition.

In our experiments, we found the efficiency of jarosite formation was noticeably retarded when EPS were stripped. The capacity of EPS to immobilize ions has been extensively reported.[36,37] The reacting assembly of EPS supplies active sites to anchor and accumulate the dissolved aqueous ions, facilitating the precipitation and nucleation of minerals by reducing the activation energy barriers.[38,39] All these facts indicate that the EPS plays a key role in providing nucleation sites to bind metal ions and facilitating the generation of larger mineral aggregates. Besides, the process was impacted by the pH value

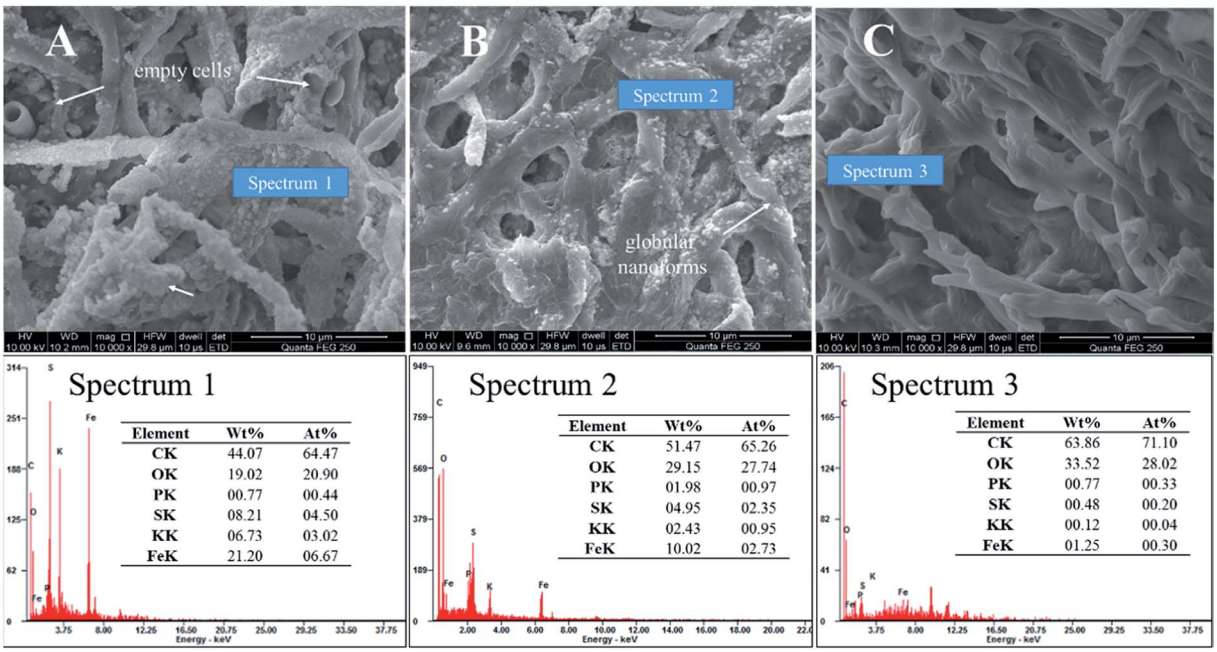

Fig. 6 SEM micrographs showed the effect of EPS on biomineralization (pH 2.5, 2nd day): (A) autoclaved method; (B) ultrasonic method; (C) comprehensive method.

obviously in this study, the unformed pellets with uneven size of biomineral were observed and the process takes place outside the cell. There is an independent process of metal ions to bind fungal surface. This is a passive formation process that could be implemented by different morphological cell surface and is on the basis of the ability of cell walls.[40] These results all indicated that the process of *P. lilacinum* promote biosynthesis of jarosite belongs to BIM. Thus, BIM plays a key role in biomineralization process in this article.

3.3 Comparison of FTIR spectrum in different biomineralization periods

The FTIR spectra presented in Fig. 7 revealed the changes of the fungal cell surfaces groups over the eleven-day biomineralization period. At twelve-hour period of biomineralization (Spectrum A), no obvious mineral precipitate could be observed. The peak allocations of EPS are as follows: the bands at 2925 and 2855 cm^{-1} vest in the asymmetric stretching of $-CH_2-$ and symmetric stretching of $-CH_2-$, respectively; the band at 1654 cm^{-1} vests in the C=O stretching in amide I group; near 1556 cm^{-1} is assigned to the C–N stretching and N–H bending in amide II group.[41,42] In the 900–1300 cm^{-1} spectral range are assigned to the phosphorylated proteins or phosphodiester group.[43] Besides, the bands at 811 and 894 cm^{-1} are assigned to Fe–OH out of-plane and in plane bending vibrations.[44] At one day period (Spectrum B), the 2855 cm^{-1} and 1745 cm^{-1} bands which were from free EPS had lost most of its intensity, indicating the existence of conformational changes. At two days period of biomineralization (Spectrum C), biomineral grown within the EPS could be observed. The appearance of new band at 1014 cm^{-1} is due to the stretching vibration of P–O–Fe bonds.[45–47] Near 1084 cm^{-1} vest in the symmetric stretching of O–P–C.[48] At four days period (spectrum D), there are well separated bands at 474 and 515 cm^{-1} are assigned to the vibration of the FeO_6 octahedron, the band at 630 cm^{-1} vest in the stretching vibration of SO_4^{2-}.[49,50]

In this experiment, by monitoring the FTIR marker bands insight was obtained in the role of the EPS to jarosite formation. We found that the FTIR spectra of the fungal cell surface groups changed with the biomineralization process, and the variation in frequency and intensity of the biofilm market bands indicated the existence of compositional and structural changes. The EPS spectrum of amide I group (1654 cm^{-1}) and amide II group (1556 cm^{-1}) turned into 1649 cm^{-1} and 1543 cm^{-1}

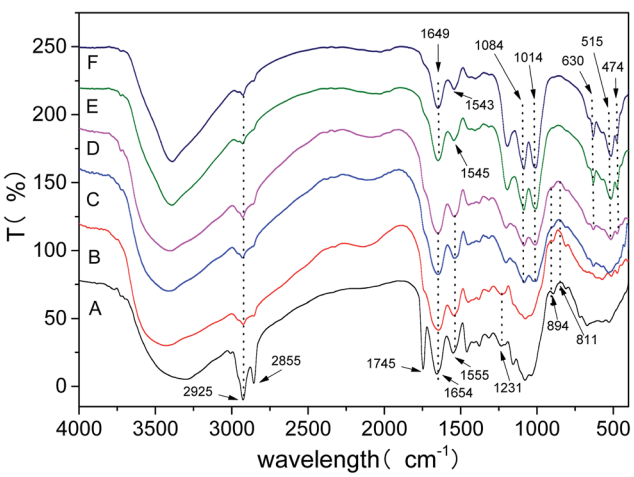

Fig. 7 FTIR spectra of different biomineralization periods (pH 2.5). Spectra A–F are at 12th hours and 1st, 2nd, 4th, 6th, 11th day, respectively.

(Spectrum F) for the EPS-jarosite complex, respectively. In the surface of attached microorganisms, the variation in intensity and frequency of amide I group has been observed and the characteristic absorption peak of biofilm formation have been observed.[43] The transform indicated that the proteins of EPS were drawn into the EPS mineralization and absorption on jarosite.[27] Besides, the band at 1231 cm^{-1} was due to the stretching vibration of P═O, which in the spectrum of bulk EPS was gradually disappeared with the mineral precipitate process (Spectrum A and B). This phenomenon also manifested that the electron concentration of the phosphorous atoms was weakened and the free PO_2^- was missing[47] Most significantly was the appearance of stretching vibrations of P–O–Fe bonds (Spectrum C–F) and the vanishment of bending vibrations of Fe–OH band (Spectrum A–D), the phenomenon was associated with the process of $Fe(OH)_3$ transformed into jarosite at the last step of de-ironing. Finally, the vibration bands of the FeO_6 octahedron and SO_4^{2-} were gradually separated with time (Spectrum D–F) that were consistent with the evolution process of the crystal structure of mineral precipitate. All of these results showed that the biomineralization might result of the existence of free P═O group acted as nuclei sites for the process of jarosite formation, possibly promoting $Fe(OH)_3$ transformed into jarosite by the formation of P–O–Fe bonds between jarosite Fe metal centers and phosphoryl groups.

4 Conclusion

Our results showed that *P. lilacinum* could obviously improve the initial rate of jarosite formation by secreting EPS and reduce dependence of biomineralization upon pH value. The free group of P═O in EPS serving as nucleation sites promoted the transformation of $Fe(OH)_3$ into $KFe_3(SO_4)_2(OH)_6$ by forming P–O–Fe bonds between phosphoryl groups and Fe^{3+} metal centers in jarosite. The information got in this research is of important significance for understanding the mechanisms of biomineralization mediated by fungi in acid environment. In the near future, we will look deeper into the role of key components of EPS in the biomineralization process.

Conflicts of interest

There are no conflicts to declare.

Acknowledgements

This work was supported by the National Natural Science Foundation of China (No. 31470230, 51320105006, 51604308), the Youth Talent Foundation of Hunan province of China (2017RS3003), Natural Science Foundation of Hunan Province of China (No.2018JJ2486).

References

1 J. R. Young, S. A. Davis, P. R. Bown and S. Mann, *J. Struct. Biol.*, 1999, **126**, 195.
2 I. A. Aksay, M. Trau, S. Manne, I. I. Honma, N. Yao, L. Zhou, P. Fenter, P. M. Eisenberger and S. M. Gruner, *Science*, 1996, **273**, 892–898.
3 K. W. Bladh, *Econ. Geol.*, 1982, **77**, 176–184.
4 M.-C. Xia, P. Bao, A. J. Liu, S.-S. Zhang, T.-J. Peng, L. Shen, R.-L. Yu, X.-L. Wu, J.-K. Li, Y.-D. Liu, M. Chen, G.-Z. Qiu and W.-M. Zeng, *J. Biosci. Bioeng.*, 2018, **126**(1), 78–87.
5 J. M. Bigham, U. Schwertmann, S. J. Traina, R. L. Winland and M. Wolf, *Geochim. Cosmochim. Acta*, 1996, **60**, 2111–2121.
6 D. Craw, *Miner. Deposita*, 2006, **41**, 357–368.
7 G. Klingelhöfer, R. V. Morris, B. Bernhardt, C. Schröder, D. S. Rodionov, P. A. de Souza Jr, A. Yen, R. Gellert, E. N. Evlanov and B. Zubkov, *Science*, 2004, **306**, 1740–1745.
8 W. H. Farrand, T. D. Glotch, J. W. Rice Jr, J. A. Hurowitz and G. A. Swayze, *Icarus*, 2009, **204**, 478–488.
9 M. Oggerin, F. Tornos, N. Rodriguez, C. del Moral, M. Sanchez-Roman and R. Amils, *Environ. Microbiol.*, 2013, **15**, 2228–2237.
10 S. K. Das, J. Liang, M. Schmidt, F. Laffir and E. Marsili, *ACS Nano*, 2012, **6**, 6165–6173.
11 B. Ouyang, X. Lu, H. Liu, J. Li, T. Zhu, X. Zhu, J. Lu and R. Wang, *Geochim. Cosmochim. Acta*, 2014, **124**, 54–71.
12 G. M. Gadd, *Microbiology*, 2010, **156**, 609–643.
13 T. J. Beveridge, *Annu. Rev. Microbiol.*, 1989, **43**, 147.
14 M. Oggerin, N. Rodríguez, M. C. Del and R. Amils, *Res. Microbiol.*, 2014, **165**, 719.
15 S. Ziegler, S. Ackermann, J. Majzlan and J. Gescher, *Environ. Microbiol.*, 2009, **11**, 2329–2338.
16 N. Lazaroff, W. Sigal and A. Wasserman, *J. Appl. Environ. Microbiol.*, 1982, **43**, 924.
17 T. R. R. Bontognali, J. A. Mckenzie, R. J. Warthmann and C. Vasconcelos, *Terra Nova*, 2014, **26**, 72–77.
18 A.-M. P. Louis, H. Yu, S. L. Shumlas, B. Van Aken, M. A. A. Schoonen and D. R. Strongin, *Environ. Sci. Technol.*, 2015, **49**, 7701–7708.
19 M. Oggerin, F. Tornos, N. Rodríguez, C. D. Moral, M. Sánchez-Román and R. Amils, *Environ. Microbiol.*, 2013, **15**, 2228–2237.
20 C. S. Chan, G. D. Stasio, S. A. Welch, M. Girasole, B. H. Frazer, M. V. Nesterova, S. Fakra and J. F. Banfield, *Science*, 2004, **303**, 1656–1658.
21 L. Fang, Q. Huang, X. Wei, W. Liang, X. Rong, W. Chen and P. Cai, *Bioresour. Technol.*, 2010, **101**, 5774–5779.
22 R. Yu, C. Hou, A. Liu, T. Peng, M. Xia, X. Wu, L. Shen, Y. Liu, J. Li, F. Yang, G. Qiu, M. Chen and W. Zeng, *Hydrometallurgy*, 2018, **176**, 97–103.
23 K. M. McGrath, *Adv. Mater.*, 2001, **13**, 989–992.
24 D. Couchourel, C. Escoffier, R. Rohanizadeh, S. Bohic, G. Daculsi, Y. Fortun and M. Padrines, *J. Inorg. Biochem.*, 1999, **73**, 129–136.
25 C. A. Andrew, E. Khor and G. W. Hastings, *Biomaterials*, 1998, **19**, 1309–1316.
26 T. R. R. Bontognali, C. Vasconcelos, R. J. Warthmann, S. M. Bernasconi, C. Dupraz, C. J. Strohmenger and J. A. Mckenzie, *Sedimentology*, 2010, **57**, 824–844.

27 L. Fang, Y. Cao, Q. Huang, S. L. Walker and P. Cai, *Water Res.*, 2012, **46**, 5613.
28 H. Tamura, K. Goto, T. Yotsuyanagi and M. Nagayama, *Talanta*, 1974, **21**, 314–318.
29 A. S. Gong, C. H. Bolster, M. Benavides and S. L. Walker, *Environ. Eng. Sci.*, 2009, **26**, 1523–1532.
30 J. E. Jablonski, T. J. Fu, L. S. Jackson and S. M. Gendel, *J. AOAC Int.*, 2010, **93**, 213–220.
31 H.-j. Li, H.-y. Yang and G.-b. Chen, *Trans. Nonferrous Met. Soc. China*, 2016, **26**, 557–564.
32 U. Schwertmann and R. M. Cornell, *The Iron Oxides*, Wiley-CH Verlag GmbH, 2007.
33 L. I. Hai-Jun, H. Y. Yang and G. B. Chen, *Trans. Nonferrous Met. Soc. China*, 2016, **26**, 557–564.
34 D. K. Nordstrom, D. W. Blowes and C. J. Ptacek, *Appl. Geochem.*, 2015, **57**, 3–16.
35 M. Yadav, S. Kumar, R. R. Sinha, I. Bahadur and E. E. Ebenso, *J. Mol. Liq.*, 2015, **211**, 135–145.
36 A. M. Marqués, R. Bonet, M. D. Simon-Pujol, M. C. Fusté and F. Congregado, *Appl. Microbiol. Biotechnol.*, 1990, **34**, 429–431.
37 J. A. Scott and S. J. Palmer, *Biotechnol. Lett.*, 1988, **10**, 21–24.
38 K. O. Konhauser, *Earth-Sci. Rev.*, 1998, **43**, 91–121.
39 S. Mann, *Nature*, 1988, **332**, 119–124.
40 M. U. Mera, M. Kemper, R. Doyle and T. J. Beveridge, *J. Appl. Environ. Microbiol.*, 1992, **58**, 3837.
41 B. Cao, B. Ahmed, D. W. Kennedy, Z. Wang, L. Shi, M. J. Marshall, J. K. Fredrickson, N. G. Isern, P. D. Majors and H. Beyenal, *Environ. Sci. Technol.*, 2011, **45**, 5483–5490.
42 J. Wei, A. Saxena, B. Song, B. B. Ward, T. J. Beveridge and S. C. B. Myneni, *Langmuir*, 2004, **20**, 11433–11442.
43 A. Adamou, G. Manos, N. Messios, L. Georgiou, C. Xydas and C. Varotsis, *Bioresour. Technol.*, 2016, **214**, 852–855.
44 H. D. Ruan, R. L. Frost and J. T. Kloprogge, *Spectrochim. Acta, Part A*, 2001, **57**, 2575–2586.
45 A. Omoike, J. Chorover, K. D. Kwon and J. D. Kubicki, *Langmuir*, 2004, **20**, 11108–11114.
46 J. Sheals, A. Staffan Sjöberg and P. Persson, *Environ. Sci. Technol.*, 2002, **36**, 3090.
47 B. C. Barja, a. M. Isabel TejedorTejedor and M. A. Anderson, *Langmuir*, 1999, **15**, 2316–2321.
48 M. Cagnasso, V. Boero and J. Chorover, *Colloids Surf., B*, 2010, **76**, 456–467.
49 N. Lazaroff, L. Melanson, E. Lewis, N. Santoro and C. Pueschel, *Geomicrobiol. J.*, 1985, **4**, 231–268.
50 D. Baron and C. D. Palmer, *Geochim. Cosmochim. Acta*, 1996, **60**, 185–195.

